Small-Angle X-ray Scattering and Rheological Characterization of Alginate Gels. 3. Alginic Acid Gels

Kurt Ingar Draget,[†] Bjørn T. Stokke,*[,‡] Yoshiaki Yuguchi,[§,||] Hiroshi Urakawa,[§] and Kanji Kajiwara[§,⊥]

NOBIPOL, Department of Biotechnology, The Norwegian University of Science and Technology, NO-7491 Trondheim, Norway, NOBIPOL, Department of Physics, The Norwegian University of Science and Technology, NO-7491 Trondheim, Norway, and Faculty of Engineering and Design, Kyoto Institute of Technology, Matsugasaki, Sakyo-ku, Kyoto 606-8585, Japan

Received April 7, 2003; Revised Manuscript Received July 29, 2003

Alginic acid gels were studied by small-angle X-ray scattering and rheology to elucidate the influence of alginate chemical composition and molecular weight on the gel elasticity and molecular structure. The alginic acid gels were prepared by homogeneous pH reduction throughout the sample. Three alginates with different chemical composition and sequence, and two to three different molecular weights of each sample were examined. Three alginate samples with fractions of guluronic acid residues of 0.39 (LoG), 0.50 (InG), and 0.68 (HiG), covering the range of commercially available alginates, were employed. The excess scattering intensity I of the alginic acid gels was about 1 order of magnitude larger and exhibited a stronger curvature toward low q compared to ionically cross-linked alginate. The $I(q)$ were decomposed into two components by assuming that the alginic acid gel is composed of aggregated multiple junctions and single chains. Time-resolved experiments showed a large increase in the average size of aggregates and their weight fraction within the first 2 h after onset of gelling, which also coincides with the most pronounced rheological changes. At equilibrium, little or no effect of molecular weight was observed, whereas at comparable molecular weights, an increased scattering intensity with increasing content of guluronic acid residues was recorded, probably because of a larger apparent molecular mass of domains. The results suggest a quasi-ordered junction zone is formed in the initial stage, followed by subsequent assembling of such zones, forming domains in the order of 50 Å. The average length of the initial junction zones, being governed by the relative fraction of stabilizing G-blocks and destabilizing alternating (MG) blocks, determines the density of the final random aggregates. Hence, high-G alginates give alginic acid gels of a higher aggregate density compared to domains composed of loosely packed shorter junction zones in InG or LoG system.

1. Introduction

Alginates are regarded as a family of unbranched polysaccharides consisting of (1→4) linked β-D-ManA (M) and α-L-GulA (G) residues in different proportions and varying in sequence.[1,2] Alginate gelling by ionotropic cross-linking using multivalent ions has been known and exploited for several decades. In particular, the mild gelling conditions for the Ca^{2+} induced sol/gel transition has proven compatible with living cells and tissues, and alginates have therefore gained high popularity as an immobilization matrix in such systems.[3] The structure of the junction zones induced by divalent ions interacting selectively with the G-residues is commonly described in a model referred to as the egg-box model.[4−6] A local structural change induced by Ca^{2+} was observed by small-angle X-ray scattering for the alginates with various chain lengths and residue sequences, and the correlation between the local structure deduced from small-angle X-ray scattering and rheological properties has been discussed in the preceding papers in this series.[7,8]

It is also known that alginates may undergo a sol/gel transition upon lowering the pH below the pK_a value of the uronic acid residues.[9,10] A detailed molecular description of the structural organization of the alginic acid gels is as important for pharmaceutical applications as knowledge on ionotropic gels is for immobilization purposes. One report[9] describes the fundamentals of alginic acid gel formation with a focus on the influence of alginate chemical composition and molecular weight on rheological properties associated with gelation. It was shown that an increased fraction of homopolymeric G-blocks yielded gels with higher shear modulus. This is similar to the influence of residue sequence on gel properties of ionitropic alginate gels using divalent ions displaying selectivity for guluronic acid. The mechanism of gel formation under acidic conditions has additional facets than for ionotropic gels because the presence of homopolymeric M-blocks in alginates also creates stable junctions,

* To whom correspondence should be addressed.
[†] Department of Biotechnology, The Norwegian University of Science and Technology.
[‡] Department of Physics, The Norwegian University of Science and Technology.
[§] Kyoto Institute of Technology.
[||] Present address: National Institute of Advanced Industrial Science and Technology, AIST, 2217-14 Hayashi-cho, Takamatsu, Kagawa 761-0395, Japan.
[⊥] Present address: Ohtsuma Women's University, Faculty of Home Economics, 12 Sanban-cho, Chiyoda-ku, Tokyo 102-8357, Japan.

10.1021/bm034105g CCC: $25.00
Published on Web 09/05/2003

Table 1. Chemical Composition and Sequence and Intrinsic Viscosity (in 0.1 M NaCl) of the Alginate Samples Used in This Study[a]

alginate source	F_G	F_M	F_{GG}	$F_{GM,MG}$	F_{GGG}	[η] mL/g	$M_w/10^3$ g mol^{-1}	sample designation
A. nodosum	0.39	0.61	0.23	0.16	0.17	740	230	LoG_{230}
L. hyperborea leaf	0.51	0.49	0.33	0.16	0.28	500	155	InG_{155}
	0.51	0.49	0.38	0.11	0.33	760	240	InG_{240}
	0.49	0.51	0.32	0.17	0.27	1420	455	InG_{455}
L. hyperborea stipe	0.68	0.32	0.52	0.16	0.47	520	160	HiG_{160}
	0.69	0.31	0.57	0.12	0.52	720	225	HiG_{225}
	0.71	0.29	0.52	0.19	0.47	1440	465	HiG_{465}

[a] *F* assigns the different fractions of monomer and monomer sequences found in these samples by NMR spectroscopy.

although to a lesser extent than G-blocks. It is also found that the alginates rich in not strictly alternating MG-sequences do not yield strong gels, indicating that these types of the sequences do not contribute to junctions under acidic conditions and thus perturb gel formation. These equilibrium results have later been verified under nonequilibrium conditions where alginic acid gels were allowed to swell and partially dissolve at pH just above the pK_a value of the uronic acid residues.[10] An enrichment of MG and M sequences in the leached material compared to the average of the material used to make gel was observed. Another characteristic feature of the acid gel is that the elasticity of the acid gel does not depend on the history of gel formation, indicating that these gels are closer to an equilibrium state than the ionotropic gels.[9] Furthermore, the acid gels are more turbid, and the elasticity of the high-G acid gel increases with molecular weight over a broader range of molecular weights compared to the ionically cross-linked alginate gels.

The aim of this work is to reveal possible differences in the local structure of the gels underlying the influence of the primary structure of the alginates on the macroscopic gel properties and to compare the gel formation mechanism of acid gel with ionotropic Ca-alginate gel. The focus is on the differences in the local structural dimensions, as observed by small-angle X-ray scattering (SAXS),[11] between the two types of gel. Structural differences, and hence different mechanisms for junction formation, could be expected because the acid gel appears considerably more turbid than the ionically cross-linked gels. Another motivation was to study the correlation between time-resolved SAXS data with the rheological sol/gel transition of the alginic acid gels to observe if any structural change takes place on a local molecular scale prior to any macroscopical sol/gel transition.

2. Material and Methods

2.1. Alginate Samples. FMC Biopolymer A/S, Drammen, Norway, kindly provided alginate samples isolated from different types of seaweeds. The chemical composition and sequence, the intrinsic viscosity ([η]; mL/g) in 0.1 M NaCl at 20 °C, and the weight average molecular weight (M_w) of the different samples are shown in Table 1. Chemical composition and sequence specified in terms of the mean fraction of selected diad and triads of the residues, were determined by high-field ^{1}H NMR analysis as described earlier.[12] M_w was calculated using the experimentally determined [η] and the Mark−Houwink equation [η] (mL/g) = 4.84×10^{-3} $M_w^{0.97}$ (ref 7). The three-letter acronym introduced previously[7] was used to depict each sample (Table 1). The added sub-scripts describe the weight average molecular weight in units of kg/mol. Alginate stock solutions (20 mg/mL) were prepared by dissolving 1.0 g of alginate in 50 mL of deionized water, stirred overnight at room temperature, and filtered (1.2 and 0.7 μm pore size (Millipore)) prior to use.

2.2. Preparation of the Alginic Acid Gels. Alginic acid gels were prepared as described earlier.[9] A controlled lowering of the pH within a 10 mg/mL Na-alginate solution was achieved by adding 0.8 M slowly hydrolyzing D-glucono-δ-lactone (GDL). This amount of GDL gives a final pH $\leq$ 2.5 and has been shown to produce alginic acid gels where the apparent gel strength starts to level off with respect to amount of GDL added.[9] The samples were degassed prior to loading them into the sample cells for the SAXS experiments.

2.3. Rheological Characterization. Dynamic rheological characterization of the alginate solutions and the alginic acid gels were performed by recording the frequency dependence of $G'(\omega)$ and $G''(\omega)$ at $T = 20$ °C using a Bohlin VOR (Lund, Sweden) or a Reologica Stresstech general purpose rheometer. The VOR was equipped with a torsion bar with torsional stiffness 4.0 g cm. The alginic acid gels were characterized within a serrated plate-plate measuring geometry, and a 5 mPas silicone oil was used to seal the samples to avoid evaporation during the extended characterization of the gelation. The frequency dependence of the alginate solutions was determined in a double-gap measuring geometry. Gelling kinetics was characterized by determination of G' and G'' every 3 min for up to 24 h after adding GDL to initiate gelling.

2.4. Small-Angle X-ray Scattering. SAXS (small-angle X-ray scattering) was observed from alginic acid gels with the SAXES equipment installed at BL-10C in the Photon Factory, Tsukuba, Japan.[13] The details of the equipment adjustment and experimental procedure are described previously.[7,8] Briefly, a monochromatic X-ray beam with $\lambda = 1.488$ Å obtained using a double-crystal monochromator of the incident X-ray from the synchrotron was focused to the sample cell using a bent focusing mirror. A one-dimensional position sensitive proportional counter (PSPC) of an effective length of 160 mm was used to determine the scattered intensity by the gels. The exact camera length was calibrated with the diffraction peaks of collagen fiber. The range of magnitude of the scattering vector q was from $q = 0.014$ to 0.4 Å^{-1}. The scattering profiles were obtained for gels equilibrated for 20−24 h after the onset of gelling, using 15 min data accumulation time. Because of a rapid sol/gel transition of the alginic acid gel, a 2 min data accumulation

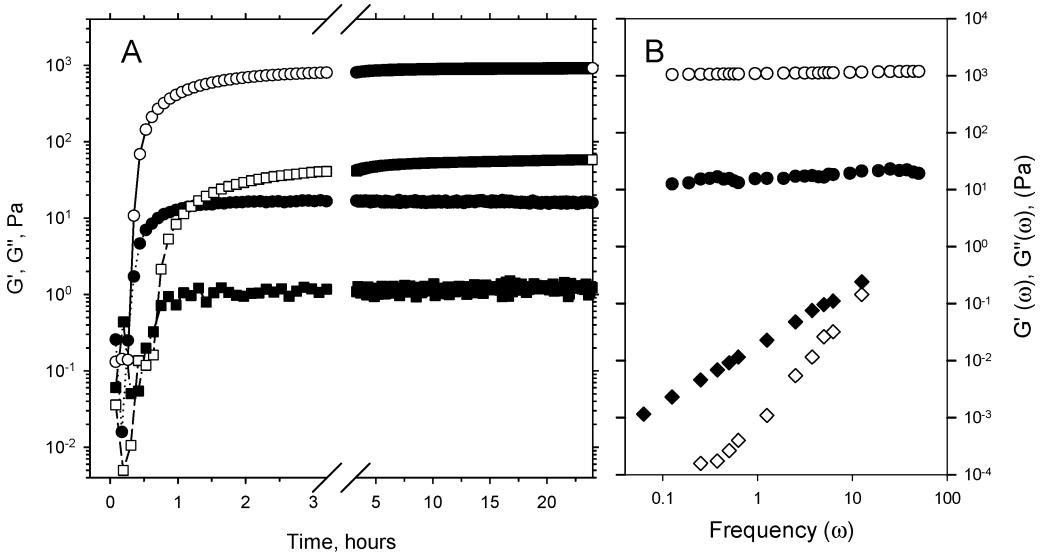

Figure 1. (A) Development of G' (open symbols) and G'' (closed symbols) for the time-resolved formation of alginic acid gels made from 10 mg/mL HiG_{160} (○, ●) and 10 mg/mL InG_{155} (□, ■). (B) Changes in G′ (open symbols) and G″ (closed symbols) as function of frequency going from a 10 mg/mL Na-alginate solution (◇, ◆) to its respective alginic acid gel (○, ●) of HiG_{160}.

Table 2. Summary of Changes in G' and G'' at $\omega = 6.28\ s^{-1}$ of 10 mg/mL Alginic Acid Gels

alginate		initial		24 h gel	
sample	[η] mL/g	G' (Pa)	G'' (Pa)	G' (Pa)	G'' (Pa)
LoG_{230}	740	0.09	0.26	13	1.2
InG_{155}	500	0.036	0.061	64	1.3
InG_{240}	760	0.12	0.35	194	2.9
InG_{455}	1420	0.40	2.3	289	4.6
HiG_{160}	520	0.13	0.26	930	16.2
HiG_{225}	720	0.06	0.32	2470	10.7
HiG_{465}	1440	0.27	0.99	2940	27.9

time was allowed to each frame in the time-resolved SAXS measurements during the course of gelling. Excess X-ray scattering was recorded as the difference between each gel and its solvent in the same sample cell.

3. Results and Discussion

3.1 Rheology. The transition from solution to acid gel made from two of the alginate samples in this study is presented as the observed change of dynamic moduli with time in Figure 1. A very rapid transition is observed where the apparent equilibrium is reached within the first 2 h. Both the storage, G', and loss, G'', modulus observed during gelling of both alginate samples appear to increase in parallel within this time regime, and both dynamic moduli become nearly independent of time after approximately 3 h. Even though both G' and G'' increase during transition, a difference of almost 2 orders of magnitude is observed at equilibrium. Figure 1a also shows that G' and G'' of the acid induced gel of *L. hyperborea* stipe (high-G alginate, HiG) are significantly larger than those of the acid induced gel of *L. hyperborea* leaf (intermediate-G alginate, InG). This difference highlights the importance of chemical composition at comparable degrees of polymerization. A summary of the determined changes in G' and G'' from solution to gel of the different alginates is presented in Table 2.

The data (Table 2) show that the average molecular weight as well as the chemical composition and sequence have a profound effect on the bulk rheological properties at apparent equilibrium. For both InG and HiG, there seem to be an almost linear relationship between the average molecular weight and the dynamic storage modulus G'. The most noticeable effect is, however, exposed when the content of guluronic acid residues is changed. At comparable average molecular weights, an increase in G' in excess of 100 times is observed when the fraction of guluronic acid residues is increased from 0.4 to 0.7.

Figure 1b shows the frequency dependence of G' and G'' of one of the alginate samples included in this study, prior to and after gelling. The alginate solution prior to acid gel formation is predominantly a viscoelastic liquid with G' being generally lower and more frequency dependent than G'' within the given range of ω. After gelling, the system has changed into a predominantly viscoelastic solid with G' being less frequency dependent and larger than G'' over the entire range of ω studied. Additionally, an apparent equilibrium has been reached as indicated by a frequency independent storage modulus.

3.2. Small-Angle X-ray Scattering. *Molecular Weight Dependence.* Figure 2 shows the intensity $I(q)$ of excess scattering as a function of the magnitude of scattering vector q from alginic acid gels made from *L. hyperborea* stipe (HiG) at different degrees of polymerization. The scattering profiles of the alginate acid gels prepared from *L. hyperborea* leaf (InG) (data not shown) revealed only smaller chain length dependence. The magnitude of the scattering vector q is given in terms of the scattering angle θ and the wavelength of an incident light λ as

$$q = (4\pi/\lambda)\sin(\theta/2) \quad (1)$$

The observed excess scattering intensities of these gels are characterized by a sharp increase below $q = 0.10\ Å^{-1}$ with the highest intensities at the smallest accessible q, indicating the presence of large aggregates. Compared to the scattering profiles for Ca-alginate gels presented earlier,[7] there is a typical intensity increase at low q of about 1 order of

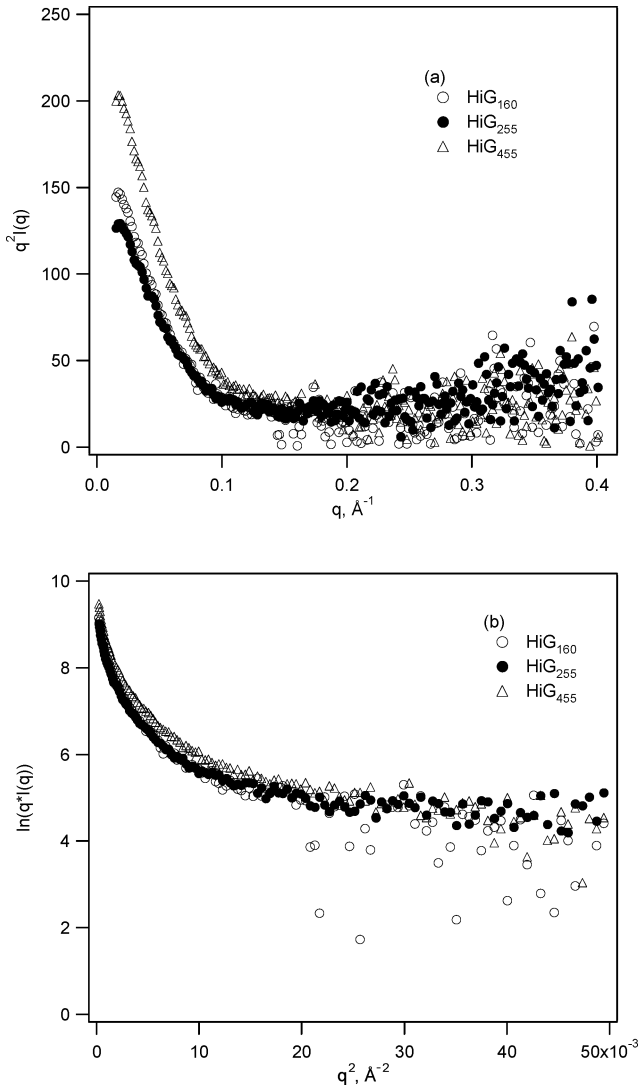

Figure 2. Excess small-angle-X-ray scattering profiles for alginic acid gels made from 10 mg/mL HiG alginate (a and b) varying the average molecular weights. The figure shows Kratky plots (a) and Guinier cross-sectional plots (b).

magnitude. This corresponds well to visual observations of alginic acid gels being more turbid because of higher degrees of association within the acid gel network. Only small systematic changes in excess X-ray scattering as a function of molecular weight were observed. This indicates that the observed increase in G' with chain length (Table 2) is due both to a reduction of sol and loose-end fractions and to the difference in local network structure with a larger cross-linking domain formed at the largest molecular weight.

The so-called cross-sectional Guinier plots of the data, ln-(q*I(q)) versus q^2 (Figure 2b) may allow an extraction of the multiplicity of junction zones from the large negative tangential slopes corresponding to the cross-sectional radius of gyration of rodlike objects.[14] Here, a junction zone implies a domain composed of quasiordered alginic acid chains laterally associated similar, but not necessarily of equal geometrical detail, to that specified for Ca-alginate gels. However, the actual cross-sectional Guinier plots exhibit a marked curvature for acid gels, making an estimation of junction multiplicity in terms of a single cross-sectional dimension almost impossible. This may be due to the broad cross-sectional size distribution of the junction zone multiplicity. As a very rough estimate ($q^2 \in (0.001-0.01)$ Å^{-2}), all samples in both the HiG and InG series give cross-sectional values between 60 and 70 Å. Within these levels of junction multiplicity, which might also distribute broadly, it is doubtful if the mathematical model for the deduction of multiplicity is still valid. The cross-sectional radius of gyration of the model cylinders may be comparable to their length and/or the size distribution of junction multiplicity is too broad. The absence of a clearly identifiable correlation peak observed for alginates dissolved in water (data not shown) most probably reflect the rapid hydrolysis of GDL to yield a sufficient ionic strength suppressing this before data could be collected.

A better approach is therefore to try to decompose the scattering curve into two components. This can be achieved based on the assumption that the acid gel is composed of aggregated multiple junctions and single chains representing the two components. Here the scattering from aggregated multiple junctions can be given in terms of the Debye−Bueche formula for random aggregates[15] as

$$I_{DB}(q) \approx \frac{k_1}{(1 + a^2q^2)^2} \tag{2}$$

where a provides a measure for the average size of aggregates. The scattering from a single chain may follow the Ornstein−Zernicke function specified by a correlation length ξ[16] given by

$$I_{OZ}(q) \approx \frac{k_2}{1 + \xi^2q^2} \tag{3}$$

Parameters k_1 and k_2 in eqs 2 and 3 are the constants including the polymer concentration and scattering density. A total scattering profile is given by the sum of those two terms as

$$I_{total}(q) = I_{DB}(q) + I_{OZ}(q) \tag{4}$$

It was assumed that there was no interference between the two components in this model. In the two-component model, $I_{DB}(0)$ and $I_{OZ}(0)$ provide a rough estimate for apparent molecular masses of respective components, although the values are dependent on the scattering density in each component. Although log $I(q)$ vs log(q) shows linearity for a limited region of q, this region of q is generally so small that an equally good fit of a scaling law, $I(q) \sim q^{-D}$ valid for a fractal gel,[17] could not be obtained. These models appear therefore not to yield a good model for the alginate acid gels.

Figure 3, parts a−c, shows the transitional, time-resolved scattering intensities of an acid gel made from the HiG_{160} sample. The relative change in scattering intensity during this sol/gel transition covers more than 2 orders of magnitude with the largest change at low scattering vectors (q) taking place within the first 2 h. This time frame corresponds to the time where the largest change in G' and G'' was observed (Figure 1). Between 2 and 24 h, the net result seems to be more or less a parallel shift in scattering intensity as function of q, suggesting a merging of scattering domains of all sizes into steadily increasing structures. To make the discussion

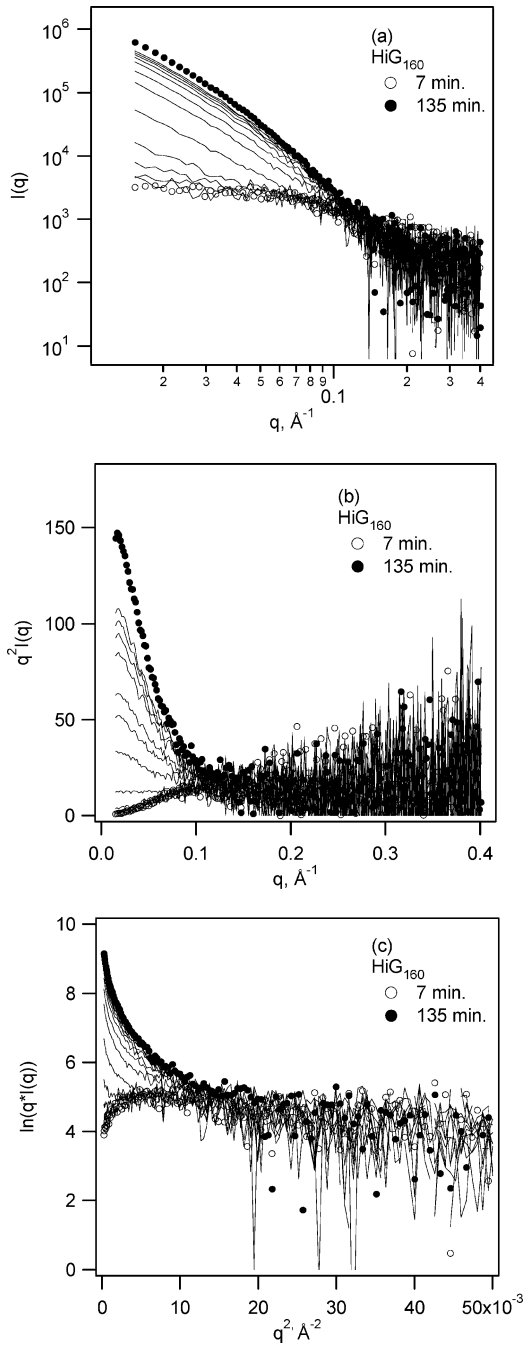

Figure 3. Time-resolved excess small-angle-X-ray scattering profiles for alginic acid gels made from 10 mg/mL HiG_{160} in terms of the double-logarithmic plots (a), Kratky plots (b), and cross-sectional Guinier plots (c). Measuring intervals after addition of D-glucono-δ-lactone: 7 (○), 11, 15, 19, 21, 23, 25, 27, 31, 35, 39, 43, 47, and 135 (●) min.

more quantitative, we have decomposed the scattering profiles into two components according to eq 4. Figure 4 shows the results of the decomposed scattering profiles into two components given by eqs 2 and 3, respectively, at the time 135 min after initiating gelation. Here the correlation length ξ is fixed to 10 Å as determined 7 min after initiation the pH reduction (a starting frame), because the range becomes insufficient at the later stage of gelling for the scattering profile to be represented by eq 3. It was further assumed that there was no change of a single chain conformation during gelling. Two parameters emerge from the two-component analysis, where a specifies a measure

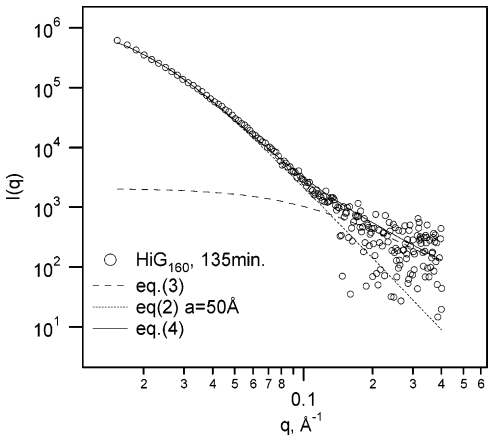

Figure 4. Decomposed scattering profiles from 10 mg/mL HiG_{160} according to eq 4.

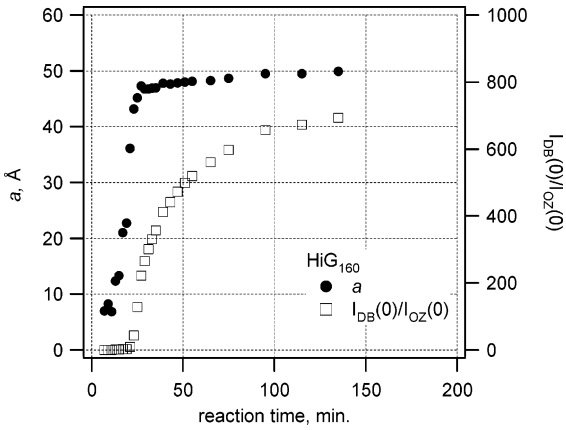

Figure 5. Time evolution of a (a measure for the size of a domain formed by linked short junction zones) and $I_{DB}(0)$ (a measure for an apparent molecular mass of a domain) for alginic acid gels made from 10 mg/mL HiG_{160} after addition of D-glucono-δ-lactone.

for the size of aggregated junction zones and $I_{DB}(0)$ provides a relative estimate for the apparent molecular mass of aggregated junction zones in the system. As shown in Figure 5, both a and $I_{DB}(0)$ increase with time and reach almost an equilibrium value within 2 h.

At the initial stage, the scattering profile is characterized by a rodlike behavior as confirmed by a linear part of the cross-sectional Guinier plots (Figure 3c). The rodlike behavior disappears, and the random aggregation is observed as indicated by the abrupt increase of the scattering intensity at $q \rightarrow 0$. Although the employed integration time for accumulation of scattered data causes a poor S/N ratio in the time-resolved studies, the cross-sectional radius of gyration is evaluated to be around 7 Å from the cross-sectional Guinier plots up to a certain time (approximately after 20 min) when an abrupt upturn of the scattering is observed. Because the cross-sectional radius of gyration of a single alginic chain is about 4 Å,[7] the cross-sectional radius of gyration 7 Å indicates a bundle of 3−4 chains forming a junction zone. During this period, the junction zone grows laterally as qualitatively observed from the scattering profiles. This observation indicates that the quasiordered junction zone in the acid gels would not grow so much but split into other junction zones or single chains resulting in the formation of a kind of random aggregates composed of small pieces of junction zones. The obstacle against the formation of a

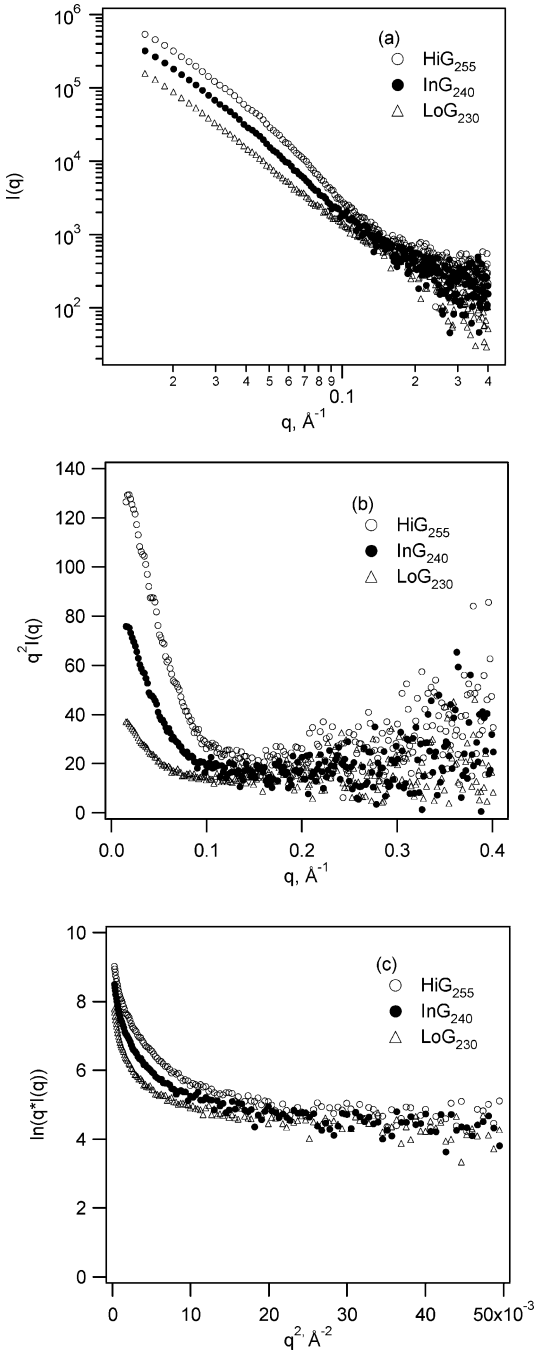

Figure 6. Excess small-angle-X-ray scattering profiles for alginic acid gels made from 10 mg/mL HiG_{225} (●), InG_{240} (△), and LoG_{230} (○) in terms of the double-logarithmic plots (a), Kratky plots (b), and cross-sectional Guinier plots (c).

quasiordered junction zone is supposed to be due to the inclusion of sequentially inhomogeneous GM-blocks in the cross-linking domain. Because the acid gel is composed of interconnected random aggregates, as opposed to well-ordered junction zones observed for Ca-alginate gels, the acid gel exhibits properties characterized by brittleness and a relatively high levels of plasticity.

Dependence of Chemical Composition. The data presented in Figures 2 and equivalent data of alginate acid gels prepared from *L. hyperborea* leaf (InG) did not reveal any substantial effects of molecular weight on scattering intensities or cross-sectional radii of gyration. The question of possible influence of chemical composition and sequence on scattering profile

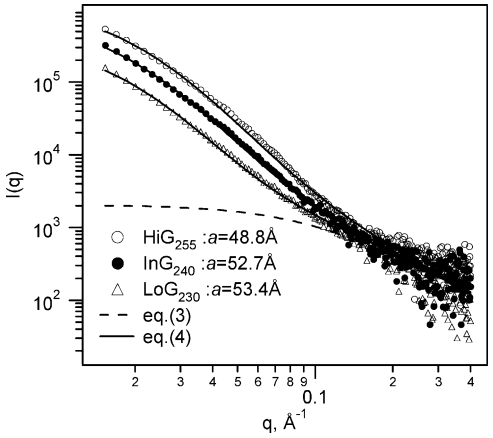

Figure 7. Decomposed scattering profiles from alginic acid gels made from 10 mg/mL HiG_{225} (●), InG_{240} (△), and LoG_{230} (○) according to eq 4.

was clearly worth a study because the rheological data at apparent equilibrium revealed large effects of these variables (Table 2). Parts a−c of Figure 6 show the double logarithmic plot, the Kratky plot, and the cross-sectional Guinier plot, respectively, of three samples with highly different chemical composition but with comparable degrees of polymerization. All three cross-sectional plots in Figure 6c exhibit large curvatures, making a single cross-sectional estimate too much of an oversimplification. Thus, we adapt two-component model as discussed above. Figure 7 shows the results of two-component analysis according to eq 4. Here the correlation length ξ is fixed to 10 Å as discussed above. Parameter a (a measure for the size of random aggregates) is evaluated to be 48.8, 52.7, and 53.4 Å respectively for HiG, InG, and LoG. Two-component analysis reveals that the evaluated value of a is comparable regardless of the chemical composition and sequence. However, the scattering intensity of $I_{DB}(q)$ at $q = 0$ becomes stronger with longer G-blocks. Here the increase of $I_{DB}(0)$ may be attributed to either a larger apparent molecular mass of aggregates or a larger number of the domain. Considering that the total polymer concentration is identical, we may conjecture that the increase of $I_{DB}(0)$ is probably due more to a larger apparent molecular mass of domains in high-G acid gel. That is, the higher domain density in high-G acid gel yields a basis for higher connectivity and thereby results in a higher elastic modulus. When we compare this observation with earlier rheological data showing alginic acid gels with a high content of guluronic acid residues to have considerably higher elastic modulus,[9] it seems reasonable to state that the more predominant viscoelastic solid behavior of high-G acid gels can be related to homopolymeric regions of guluronic acid residues being efficient building-blocks in acid gel junction formation.

To understand the chemical dependence of gel formation from the dynamic viewpoints, the time-resolved small-angle scattering was observed from the InG_{155} (Figure 8) acid gel formation in addition to HiG_{225} (Figure 3). A marked difference appears at the initial stage of gelling, where the InG_{155} system contains random aggregates, whereas the HiG_{255} system is composed mainly of quasiordered junction zones. This result indicates that hydrolysis of the added D-gluco-δ-lactone leads to junction zone formation, which

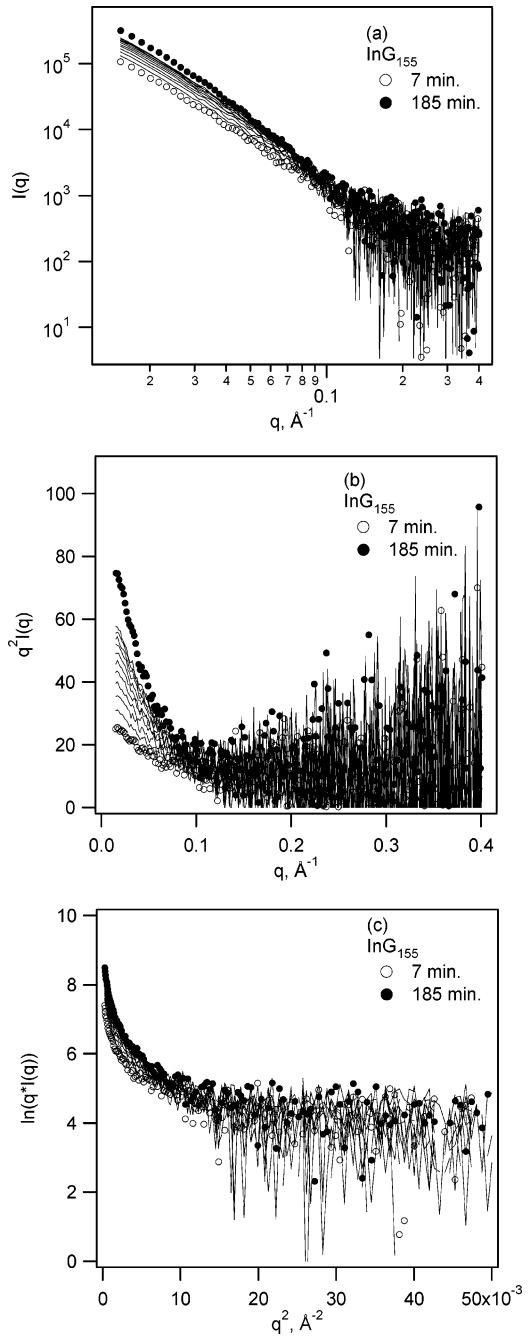

Figure 8. Time-resolved Guinier cross-sectional plots for alginic acid gels made from 10 mg/mL alginate InG_{155}. Measuring intervals after addition of D-glucono-δ-lactone: 7 (○), 11, 15, 19, 21, 23, 27, 31, 35, 39, 43, 47, 51, 55, 59, 63, 67, and 185 (●) min.

will be interrupted by the inhomogeneous MG sequence. Then a junction zone (quasiordered bundle structure) splits into several chains, and some chains may be incorporated in other junction zones. As a consequence, small pieces of junction zones are connected by short single chains and form a domain composed of small pieces of junction zones assembled in a random fashion. Those domains are linked to constitute a network, resulting in gel formation. Because high-G alginic acid is able to build longer junction zones, a domain formation is delayed and its density (an apparent molecular mass) will be higher than the domains composed of loosely packed shorter junction zones in InG or LoG system. Fit of the two-component model (eq 4) to the time-resolved $I(q)$ show a more rapid development of the a parameter for the InG_{155} sample than for HiG_{160} sample (Figures 6 and 9). The indication that a levels off (Figures 6 and 9) at a value comparable to that determined from the alginate acid gels only studying following the gel formation suggests that repeated exposure during these dynamic experiments does not induce radiation damage affecting the structure formation.

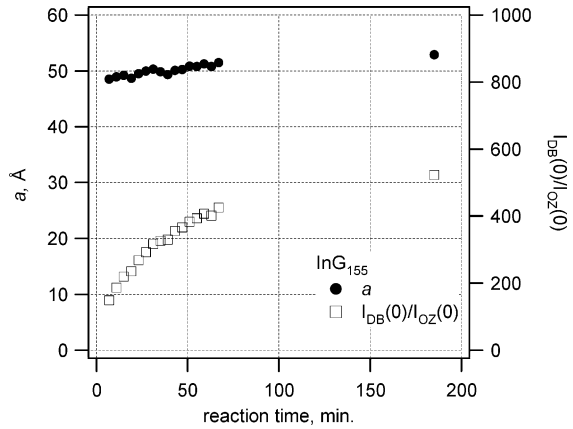

Figure 9. Time evolution of a (a measure for the size of a domain formed by linked short junction zones) and $I_{DB}(0)$ (a measure for an apparent molecular mass of a domain) for alginic acid gels made from 10 mg/mL InG_{155} after addition of D-glucono-δ-lactone.

4. Conclusion

For alginates with a high content of guluronic acid, a network formation under acidic conditions proceeds through an initial phase consisting of quasiordered junction zone composed of 3−4 laterally associated chains. This phase does not show sufficient lateral growth to support a continuous network formation sufficient for gelation. Subsequent assembling of linked junction zones takes place in the second stage, which form the domains of the size about 50 Å. Here the length of junction zones is determined by the apparent frequency of alternating GM sequences. The domains composed of randomly linked small junction zones serve as cross-linking points, and the network is formed eventually in the second stage. For alginates with intermediate content of guluronic acid, the gelation reaction proceeds too rapidly to be captured by the time-resolved SAXS studies, but a suprastructure evidence similar to the HiG samples obtained at equilibrium, indicates a similar mechanism.

The present data show that the selection of chemical composition, sequence, and chain length of the material can be used to prepare alginate acid gels with prescribed properties. These properties comprise elastic attributes, local structure, and also gelling kinetics. In this respect, naturally occurring alginates offer a basis for tailoring alginate gel properties for alginic acid gels similar to what previously is reported for Ca-alginate gels. Various properties of elasticity and local structure can be expected to be of importance in various applications such as drug delivery. Although the naturally occurring alginates offer a certain range of chemical composition and sequence, the emerging possibilities arising from using enzymatically tailored alginates by recombinantly produced C-5-mannuronan epimerases may enhance the range of alginic acid gel properties obtainable.

Acknowledgment. Part of this work was performed under the approval of the Photon Factory Advisory Committee (Proposal No. 94G 291). This work was supported by grants from Japan Society for Promotion of Science, the Ministry of Agriculture, Japan, the Ministry of Education, Science, Sports and Culture (Grant-in-Aid 07455384), the Norwegian University of Science and Technology, NTNU, the Norwegian Research Council and FMC Biopolymers a.s., Drammen, Norway. The authors gratefully acknowledge the skillful assistance by engineer Ingrid Draget.

References and Notes

(1) Moe, S. T.; Draget, K. I.; Skjåk-Bræk, G.; Smidsrød, O.; Alginate. In *Food Polysaccharides and their applications*; Stephen, E. A., Ed.; Marcel Dekker: New York, 1995; pp 245−286.
(2) Draget, K. I.; Smidsrød, O.; Skjåk-Bræk, G. Alginates from Algae. In *Biopolymers. Polysaccharides II: Polysaccharides from Eucaryotes*; De Baets, S., Vandamme, E., Steinbüchel, A., Eds.; Wiley-VCH Verlag: Weinheim, Germany, 2002; Vol. 6, pp 215−244.
(3) Smidsrød, O.; Skjåk-Bræk, G. *Trends Biotechnol.* **1990**, *8*, 71−78.
(4) Grant, G. T.; Morris, E. R.; Rees, D. A.; Smith, P. J. C.; Thom, D. *FEBS Lett.* **1973**, *32*, 195−198.
(5) Morris, E. R.; Rees, D. A.; Thom, D.; Boyd, J. *Carbohydr. Res.* **1978**, *66*, 145−154.
(6) Mackie, W.; Perez, S.; Rizzo, R. Vignon, M. *Int. J. Biol. Macromol.* **1983**, *5*, 329−341.
(7) Stokke, B. T.; Draget, K. I.; Smidsrød, O.; Yuguchi, Y.; Urakawa, H.; Kajiwara, K. *Macromolecules* **2000**, *33*, 1853−1863.
(8) Yuguchi, Y.; Urakawa, H.; Kajiwara, K.; Draget, K. I.; Stokke, B. T. *J. Mol. Struct.* **2000**, *554*, 21−34.
(9) Draget, K. I.; Skjåk-Bræk, G. Smidsrød, O. *Carbohydr. Polym.* **1994**, *25*, 31−38.
(10) Draget, K. I.; Skjåk-Bræk, G.; Christensen, B. E.; Gåserød, O.; Smidsrød, O. *Carbohydr. Polym.* **1996**, *29*, 209−215.
(11) Yuguchi, Y.; Mimura, M.; Urakawa, H.; Kajiwara, K. Network characterization of some polysaccharides observed by small-angle X-ray scattering. In *Wiley Polymer Networks Group Review Series*; Stokke, B. T., Elgsaeter, A., Eds.; John Wiley & Sons Ltd: New York, 1999; Vol. 2, pp 343−362.
(12) Grasdalen, H. *Carbohydr. Res.* **1983**, *118*, 255−260.
(13) Kajiwara, K.; Hiragi, H. Structure analysis by small-angle X-ray scattering. In *Application of synchrotron radiation to material analysis*; Saisho, H., Gohshi, Y., Eds.; Elsevier: Amsterdam, 1996; pp 353−404.
(14) Glatter, O.; Krakty, O. *Small-angle X-ray scattering*; Academic Press: New York, 1982.
(15) Debye, P.; Bueche, A. M. *J. Appl. Phys.* **1949**, *20*, 518−525.
(16) deGennes, P.-G. *Scaling concepts in polymer physics*; Cornell University Press: Itacha, NY, 1979.
(17) Dadmun, M. D.; Muthukumar, M.; Schwahn, D.; Springer, T. *Macromolecules* **1996**, *29*, 207−211.

BM034105G